Linköping University Post Print

Influence of background concentration induced field on the emission rate signatures of an electron trap in zinc oxide Schottky devices

Hadia Noor, P Klason, Sadia Muniza Faraz, Omer Nour, Qamar Ul Wahab, Magnus Willander and M Asghar

N.B.: When citing this work, cite the original article.

Original Publication:

Hadia Noor, P Klason, Sadia Muniza Faraz, Omer Nour, Qamar Ul Wahab, Magnus Willander and M Asghar, Influence of background concentration induced field on the emission rate signatures of an electron trap in zinc oxide Schottky devices, 2010, JOURNAL OF APPLIED PHYSICS, (107), 10, 103717.

http://dx.doi.org/10.1063/1.3428426 Copyright: American Institute of Physics http://www.aip.org/

Postprint available at: Linköping University Electronic Press http://urn.kb.se/resolve?urn=urn:nbn:se:liu:diva-57405

Influence of background concentration induced field on the emission rate signatures of an electron trap in zinc oxide Schottky devices

Hadia Noor, P. Klason, S. M. Faraz, 4 O. Nur, Q. Wahab, M. Willander, and M. Asqhar

(Received 12 February 2010; accepted 17 April 2010; published online 24 May 2010)

Various well-known research groups have reported points defects in bulk zinc oxide (ZnO) $[N_D]$ (intrinsic): $10^{14}-10^{17}$ cm⁻³] naming oxygen vacancy, zinc interstitial, and/or zinc antisite having activation energy in the range of 0.32-0.22 eV below conduction band. The attribution is probably based on activation energy of the level which seems not to be plausible in accordance with Vincent et al., [J. Appl. Phys. 50, 5484 (1979)] who suggested that it was necessary to become vigilant before interpreting the data attained for a carrier trap using capacitance transient measurement of diodes having N_D greater than 10^{15} cm⁻³. Accordingly the influence of background free-carrier concentration, N_D induced field on the emission rate signatures of an electron point defect in ZnO Schottky devices has been investigated by means of deep level transient spectroscopy. A number of theoretical models were tried to correlate with the experimental data to ascertain the mechanism. Consequently Poole–Frenkel model based on Coulomb potential was found consistent. Based on these investigations the electron trap was attributed to Zn-related charged impurity. Qualitative measurements like current-voltage and capacitance-voltage measurements were also performed to support the results. © 2010 American Institute of Physics. [doi:10.1063/1.3428426]

I. INTRODUCTION

Zinc oxide (ZnO) is a II-VI wide band gap (3.37 eV) semiconductor with a large exciton binding energy (60 meV), even at room temperature. ZnO possess superior physical parameters, such as high breakdown electric field strength, high thermal conductivity, high electron saturation velocity, and high radiation tolerance offer great potential in terms of power and efficiency in both photonic and electronic applications This material is famous for UV light emitters/detectors and high-power and high-temperature devices.^{1,2} In addition due to its valuable optoelectronic properties, it is a candidate for the fabrication of a dilute magnetic semiconductor with a Curie temperature higher than room temperature.³ Furthermore, ZnO is piezoelectric, biosafe and biocompatible material, and possesses deep level defects (with blessing character) that emit in the whole visible spectrum with potential of developing white light sources. Finally, ZnO plays a significant role in making socalled transparent electronics.⁵ Because of these characteristics, ZnO is now considered to be in the line of traditional semiconductors such as Si and GaAs, and it is also compatible with wide band gap semiconductors such as SiC and GaN.6

Due to residual donor defects in as-deposited ZnO,⁷ all of the above-mentioned electronic device applications depend upon the defect chemistry and electronic structure of

the material, both of which have been the subjects of recent theoretical and experimental studies. The free-carrier concentration, doping compensation, minority carrier lifetime, and luminescence efficiency of such devices are directly or indirectly related to these defects.^{8–10} The source formation of these defects together with their fingerprints, such as activation energy, capture cross-section, and spatial distribution are still not understood clearly. For example, a number of studies have reported still unstable electrical properties of an electron defect level in bulk ZnO so far and the consensus on its identification is yet to be made. Some of the reports discuss the issues as what follows: Frenzel et al. 11 found an electron trap associated with Zn-interstitials having an activation energy (trap concentration) of 0.32 eV (10¹⁴ cm⁻³) below the conduction band, Wenckstern et al.² observed intrinsic donorlike defects in ZnO having an activation energy in the range of 0.30 to 0.37 eV, Frank et al. 12 demonstrated a Zn-related defect level with an ionization energy of 0.31 eV, and Auret et al. 13 reported a similar level at an energy of 0.29 eV and attributed to an oxygen vacancy. In short, the activation energy of the defect exhibits upto 40% variation, and the nature of the defect level oscillates between the Zninterstitial and the oxygen vacancy that is why no acceptable identification of the level is found. Therefore further experimentation in an effort to resolve this issue is continued. In the meantime, Diaconu et al. 14 has recently, observed that emission rates of all levels $(E_1, E_2, \text{ and } E_3)$ in cobalt (Co)doped ZnO samples decreased with increase in the background free-carrier concentration $(0.5-31.2)\times10^{17}$ cm⁻³. This observation supported with Vincent *et al.* 15 suggestion

Department of Physics, The Islamia University of Bahawalpur, Bahawalpur 63100, Pakistan

²Department of Physics, University of Gothenburg, 412 96 Gothenburg, Sweden

³IFM, Linköping University, 581 83 Linköping, Sweden

⁴Electronic Engineering, NED Engineering University, Karachi 75270, Pakistan

⁵ITN, Linköping University, Campus Norrköping, 601 74 Norrköping, Sweden

^{a)}Author to whom correspondence should be addressed. Electronic mail: magwi@itn.liu.se.

"it is necessary to become vigilant before interpreting the data attained for a carrier trap using capacitance transient measurement of diodes having N_D greater than 10^{15} cm⁻³" leads us to address the properties especially the emission rates of electron level under discussion, in n-type ZnO as a function of free-carrier concentration (N_D) of the device (ZnO).

In this paper, the influence of N_D on the emission rate signatures of an electron trap in ZnO Schottky devices has been investigated by means of deep level transient spectroscopy (DLTS). ¹⁶ A number of theoretical models were attempted on the experimental data to ascertain the mechanism, consequently, Poole–Frenkel model based on Coulomb potential was found consistent. Experimental details, results, and discussion together with conclusions are presented in Secs. II–IV, respectively.

II. EXPERIMENTAL DETAILS

The samples used in the current study were single crystal bulk-ZnO wafers, synthesized hydrothermally in the wurtzite (0001) orientation, and original size was $10 \times 10 \times 5$ mm³. These samples were obtained from ZnOrdic AB. According to the specifications provided by ZnOrdic, the samples had intrinsically n-type conductivity and the full width at half maximum measured from x-ray diffraction rocking curve for the peak at 17.74° was 20-60 arc sec. The samples were sliced into two pieces of thickness 1-mm each for characterization purposes hereafter referred as A and B. Circular (diameter ~1 mm) Schottky contacts of palladium (Pd) on sample A and B were prepared on their Zn- and O-faces, respectively, whereas, the Ohmic contacts of gold and nickel metals were deposited on the respective backside of the samples. We would like to mention here that preliminary investigation on sample A has been published¹⁷ already, therefore, in the present paper we are reporting the results altogether, focusing the DLTS data, in particular. A Keithley 6487 picoammeter is used for current-voltage (I-V) measurements, while a 7200 Boonton capacitance meter (for capacitance-voltage, C-V measurement) and a DLS-83D deep level spectrometer, Hungary (for DLTS) were used as characterization tools.

III. RESULTS AND DISCUSSION

A. I-V measurements

The typical I-V measurement data obtained from Schottky diode on sample B are shown in Fig. 1. The Schottky barrier height φ_B and ideality factor n of the diodes are calculated from the forward current, based on thermionic emission theory. I-V relationship for Schottky diode is described by the following equation: 18

$$I = I_S \left[\exp\left(\frac{qv}{nkT}\right) - 1 \right],$$

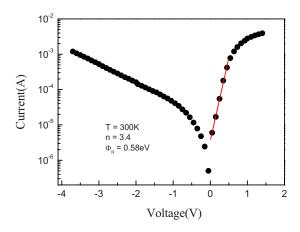


FIG. 1. (Color online) Typical *I-V* measurement of sample B, the associated quality parameters of the Schottky device are listed inside the figure.

where
$$I_S = AA^*T^2 \exp\left[\frac{-q\varphi_B}{kT}\right]$$
.

Here q, n, k, T, I_s , A, A^* , and φ_B represent charge of electron=1.6×10⁻¹⁹ C, ideality factor, Boltzmann's constant=8.617×10⁻⁵ eV K⁻¹, device temperature, saturation current, area of contact=0.0078 cm², Richardson's constant=120 m*, and barrier height, respectively. The semilog graph of the I-V (forward) data results into a straight line and its intercept and slope are incorporated in: $\varphi_B = kT/q[\ln(I_s/AA^*T^2)]$ and n=q/[kT] slope] to obtain barrier height and ideality factor, of the devices, respectively. The calculated φ_B is 0.58 eV and n is found to be 3.4. Critical discussion of the measured values φ_B and n is in the following.

According to Schottky–Mott relationship: ${}^{18}\varphi_{R} = \varphi_{m} - \chi_{s}$, where φ_m is work function of metal and χ_s is electron affinity of semiconductor. For Pd, φ_m is 5.12 eV and electron affinity of ZnO is 4.55 eV. Incorporation of these values in the relationship gives the theoretical φ_B of Pd/ZnO to be 0.57 eV which is consistent with the experimental result, nevertheless, the ideality factor n is greater than the practical limits i.e., 1-2 (diffusion-recombination nature of current, respectively). ¹⁹ This means Schottky current is recorded partially and rest of the current follows the parallel paths. Such paths may be provided by thermionic field emission (TFE), interface/surface states and/or N_D -induced barrier height lowering (to be discussed later). TFE cannot be applicable here as measurements were performed at room temperature because high temperature environment is required here so that carrier may tunnel through the thinner part of the barrier height.²⁰ However, the role of interface and/or surface states cannot be avoided. Characteristically, these states can act as carrier trap and/or recombination centers. Consequently, Schottky current is decreased and hence *n* appears as higher.

B. C-V measurements

Figure 2 shows $(1/C^2-V)$ data of the C-V measurements of sample B device maintained at room temperature measured using 1 MHz ac signal. We can see that the plot of $1/C^2$ versus V is linear in the reverse biased regime. The

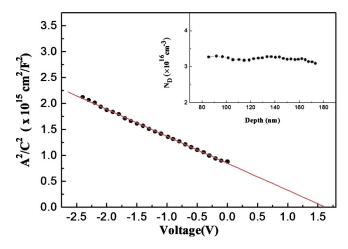


FIG. 2. (Color online) Schottky behavior of the sample B is demonstrated in $1/C^2 - V_R$, filled circles represent the experimental data and the line corresponds to the theoretical fit of the data, extrapolated to *x*-axis to yield built-in potential. The inset witnesses the uniform spatial distribution of the free-carriers in the as-deposited ZnO material.

free-carrier concentration N_D (because of intrinsic n-type conductivity) is calculated from the slope using the following relation:

$$N_D = \frac{2}{q\varepsilon \times \text{slope}}$$

and is found to be 3×10^{16} cm⁻³. The linear relationship between $1/C^2$ and V yields uniform variation in N_D data as a function junction depth as can be seen in the inset of the Fig. 2. As mentioned earlier that bulk ZnO has residual donors, we therefore, correlate N_D in our sample with such donors, details is described elsewhere. The intercept of data on the voltage axis is 1.43 V. The barrier height $(\varphi_B)_{C-V}$ and conduction band density of states N_C are calculated by following respectively: $\phi_{B(C-V)} = V_{bi} + V_O$ relations, $=kT/q\ln(N_C/N_D)$ and $N_C=2(2\pi m^*kT/h^2)^{3/2}=4.77\times 10^{18}$ cm⁻³, T=302 K. As a result, $(\varphi_B)_{C-V}$ is found to be 1.56 eV. The barrier height obtained by C-V measurements is understandably higher than that of $(\varphi_B)_{I-V}$ due to surface defects and/or interface states. 18 Recently, Dong et al. 21 and Fang et al. 22 reported similar results in intrinsically (bulk) n-ZnO Schottky diodes, and attributed the observation to the surface defects. In this perception, our results are in agreement with the literature.

C. DLTS measurements

Figure 3 demonstrates the DLTS spectra of samples A and B obtained at a reverse bias of 3 V. Filling pulse amplitude, width, and emission rate were set as 3 V, 20 μ s, and 2170 s⁻¹, respectively. Two electron traps hereafter referred as E_1 and E_2 are observed in both samples. Having been appeared at same position on the temperature scans due to both of the samples (A and B), level E_2 is qualitatively understood to exhibit the same emission rates. Consequently, the corresponding activation energy and capture cross-section of E_1 in both of the samples are found to be E_c –0.49 eV and 1.18×10^{-14} cm². On the other hand, the associated Arrhenius plots yield the quantitative difference in

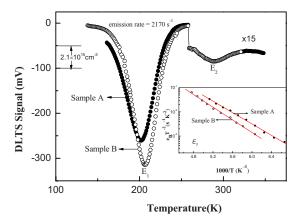


FIG. 3. (Color online) Representative DLTS scans of sample A and B to show the variation in peak position of E_1 level even measured under same measuring setup. The inset depicts its Arrhenius data in the two samples.

activation energies (capture cross sections) of E_1 level in the two samples A and B: $E_c-0.22~{\rm eV}(8.22\times10^{-17}~{\rm cm}^2)$ and $E_c-0.26~{\rm eV}(11.16\times10^{-17}~{\rm cm}^2)$, respectively (see inset of Fig. 3).

1. Level E2

Fang *et al.* observed an electron level having activation energy E_c -0.49 eV in Pd/bulk-ZnO samples. ²² Based on the comparison of the measured data of our E_2 level (activation energy, capture cross-section, and built-in potential) with those of Fang *et al.*, we therefore, correlate our level E_2 to the surface defects and boldly, the discrepancies in C-V data could be correlated with E_2 .

2. Level E₁

As describe earlier, level E_1 has different emission rate signatures in both of the samples A and B, look to be apparently same but if we do careful observation into the detail, both samples are different by: (i) face and (ii) free-carrier concentration N_D . Since face of the material is supposed to generate surface contamination, therefore, we argue that N_D could be the only element to affect the emission rates of the foresaid level. This argument is generally supported by the following reports.

- 1. Miyajima $et\ al.^{23}$ found two electron traps in gallium Ga doped ZnSe $(N_D:10^{15}-10^{18}\ {\rm cm}^{-3})$ and labeled them as trap A and B. They found that the activation energy of trap A did not vary with N_D while it was not the case with trap B, i.e., its activation energy increased from 0.4 to 0.56 eV as a function of $N_D\ (10^{18}-10^{15}\ {\rm cm}^{-3})$. In other words the activation energy of trap B increased with the decrease in free-carrier concentration. They linked trap B to the complex of Zn vacancy and Ga or the complex of interstitial Se and Ga.
- 2. According to Baber *et al.*, ²⁴ the activation energy of electron trap in some of their samples (InP) with high N_D was found to be as lower as 0.48 eV. They suggested that the so-called decrease in thermal electron emission was strongly influenced by electric field present in space charge region.
- 3. Recently, Diaconu et al. 14 observed the N_D -dependent

FIG. 4. Influence of background concentration N_D on activation energy of E_1 level, the inset shows the N_D -induced field effect on the thermal energy data of the level. Data 1 and 2 are ours and rest of the data are taken from Refs. 12, 22, and 25 for the supporting the argument described in the text.

 $(0.5-31.2) \times 10^{17}$ cm⁻³ decrease in emission rates of all levels $(E_1, E_2, \text{ and } E_3)$ in Co-doped ZnO samples.

The above reports qualitatively support our argument. In particular, various well-known groups have reported E_1 -like defect level having activation energy in the range of 0.32-0.22 eV in bulk-ZnO samples with background free-carrier concentration (10¹⁴-10¹⁷ cm⁻³). Tentatively, they attributed it to oxygen vacancy, zinc interstitial, and/or zinc antisite. The attribution is probably based on activation energy of the level which seems not to be plausible in accordance with Vincent et al. 15 who suggested that it was necessary to become vigilant before interpreting the data attained for a carrier trap using capacitance transient measurement of diodes having N_D greater than 10^{15} cm⁻³, as practically evidenced in Fig. 4 (the data include our results and those reported by other research groups 12,22,25). The information from the literature indicates that the reduction in thermal emission energy of a defect level is linked with the electric field enhanced emission. In this spirit, the inset of Fig. 4 illustrates the variation in activation energy of the level as a function of electric field generated in depletion region due to N_D ; the electric field is measured using the equation²⁶

electric field =
$$Q_{\text{dep}}/\varepsilon\varepsilon_o$$
, where $Q_{\text{dep}} = \sqrt{2qN_d\varepsilon\varepsilon_oE_g}$.

 $Q_{\rm dep}$ represents the charges in the depletion region, all the parameters bear usual meanings for the ZnO in above relations. It is clear from the figure that an electric field has a pronounced effect on the activation energy (emission rates) i.e., causing the activation energy to the lower value.

Theoretically the reduction in thermal emission energy of the carriers from the trap as a result of applied field is explained by three mechanisms: (1) Poole–Frenkel, ²⁷ (2) phonon-assisted tunneling, ^{28,29} and (3) pure tunneling. ³⁰ Mechanisms (1) and (2) are effective for only over the field range 10^4-10^6 V/cm and (3) is significant only at high fields $\geq 10^7$ V/cm. Qualitatively, Poole–Frenkel theory states that the electron band diagram is slanted and the barrier height is lowered under the applied field, therefore, the emission energy (electron) is reduced by an amount δE , however, if the electron has coupling with the suitable

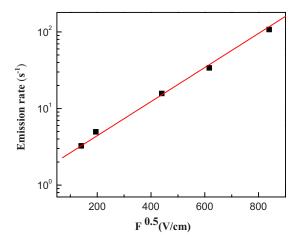


FIG. 5. (Color online) Qualitative evidence of the Poole–Frenkel mechanism on the N_D -induced variation in emission rate signatures of E_1 level.

phonon(s), then the emission energy will be even lower, and the electron will tunnel through the barrier (phonon-assisted theory). Since in our case, the reduction in thermal emission of the trap is due to N_D -induced barrier height lowering, we will therefore, only focus on Poole-Frenkel mechanism for our data. Qualitatively, a linear relationship between log (emission rate) of the trap and squared root of applied field $(F^{0.5})$ data confirms Poole–Frenkel mechanism³¹ (see Fig. 5 for evidence). Quantitatively, the effective emission energy of the carriers from the trap depends upon the type and shape of the barrier: Vincent et al. 15 and Martin et al. 30 independently proposed Coulomb potential and square well potential to fit Poole-Frenkel effect on the emission rates of the carriers. Equations (1) and (2) describe the emission rates calculated by three-dimensional Coulomb potential and square well potential exhibiting Poole–Frenkel effect

$$\frac{e_n(F)}{e_n(0)} = \frac{1}{\gamma^2} \left[e^{\gamma} (\gamma - 1) + 1 \right] + \frac{1}{2}, \quad \text{where } \gamma$$

$$= (qF/\pi \varepsilon_r \varepsilon_o)^{1/2} q/kT, \tag{1}$$

$$\frac{e_n(F)}{e_n(0)} = \frac{1}{2\gamma} (e^{\gamma} - 1) + \frac{1}{2}, \quad \text{where } \gamma = qFr/kT.$$
 (2)

Here all the constants bear usual meanings, except r in Eq. (2) represents the radius of the potential well. Using Eqs. (1) and (2), the emission rates were calculated and plotted in Fig. 6 (line) together with the experimental emission data (filled squares) for the observed trap E_1 . The result reveals that experimental data are in good agreement with the Poole–Frenkel model associated with Coulomb potential. Hence, the level E_1 is identified as a charged impurity. Furthermore, the majority of the research groups have reported Zn-related electron traps (interstitials and antisites) in intrinsically n-type ZnO material exhibiting relatively shallower energy spectrum (0.22–0.32 eV), 11,12,17,22,25 we therefore, attribute the foresaid charged impurity with Zn. This argument is consistent with the theoretical calculations revealing that Zn-interstitials are shallower than O-related defects (interstitials and antisites) in ZnO.

FIG. 6. (Color online) Theoretical fitting of the N_D -induced field emission rates (filled circles) obeying Poole–Frenkel mechanism associated with Coulomb potential (c), while square well potential (r=4.8 nm) is not consistent (s).

IV. CONCLUSION

Influence of background doping concentration induced field on an electron trap in ZnO Schottky devices has been investigated. DLTS spectrum of samples A and B with intrinsic $N_D = 3 \times 10^{16}$ and 3.44×10^{17} cm⁻³ revealed two electron traps E_1 and E_2 having activation energy (eV) (0.26 & 0.22) and (0.49 & 0.49), respectively. Level E_2 is correlated with surface states. Since various research groups found an electron level similar to E_1 in the energy range (0.22–0.32 eV) in bulk-ZnO devices with intrinsic $N_D: 10^{14}-10^{17}$ cm⁻³. The reduction in thermal energy of trap E_1 is, therefore, linked with N_D -induced barrier height lowering. In this spirit, we employed Poole-Frenkel model based on Coulomb potential on the emission rate data (ours+reported) associated with this level and found the data to be well fitted thereof. Basing on the theoretical calculations by Look et al. that Zninterstitials in ZnO are residual shallower donors in ZnO, E_1 level is identified as a charged impurity originated from Zn.

ACKNOWLEDGMENTS

The principle authors acknowledge the Higher Education Commission of Pakistan for financial support under Project No. 1019/R&D/2007 to carry out this research activity.

- ³Ü. Özgür, Y. I. Alivov, C. Liu, A. Teke, M. A. Reshchikov, S. Doğan, V. Avrutin, S.-J. Cho, and H. Morkoc, J. Appl. Phys. 98, 041301 (2005).
- ⁴M. Willander, L. L. Yang, A. Wadeasa, S. U. Ali, M. H. Asif, Q. X. Zhao, and O. Nur, J. Mater. Chem. 19, 1006 (2009).
- ⁵K. Nomura, H. Ohta, K. Ueda, T. Kamiya, M. Hirano, and H. Hosono, Science **300**, 1269 (2003).
- ⁶H. Morkoç, S. Strite, G. B. Gao, M. E. Lin, B. Sverdlov, and M. Burns, J. Appl. Phys. **76**, 1363 (1994).
- ⁷D. C. Look, J. W. Hemsky, and J. R. Sizelove, Phys. Rev. Lett. **82**, 2552 (1999).
- ⁸M. Lannoo and J. Bourgoin, Point Defects in Semiconductors I: Theoretical Aspects (Springer-Verlag, Berlin, 1981); Point Defects in Semiconductors II: Experimental Aspects (Springer-Verlag, Berlin, 1983).
- ⁹S. T. Pandelides, *Deep Centers in Semiconductors: A State-of-the-Art Approach*, 2nd ed. (Gordon and Breach Science Publishers, Yverdon, Switzerland, 1992).
- ¹⁰M. Stavola, *Identification of Defects in Semiconductors*, Semiconductors and Semimetals Vol. 51B (Academic Press, San Diego, USA, 1999).
- ¹¹H. Frenzel, H. V. Wenckstern, A. Wriber, H. Schmidt, G. Biehne, H. Hochmuth, M. Lorenz, and M. Grundmann, Phys. Rev. B 76, 035214 (2007).
- ¹²T. Frank, G. Pensl, R. Tena-Zaera, J. Zúñiga-Pérez, C. Martínez-Tomas, V. Múñoz-Sanjosé, T. Ohshima, H. Itoh, D. Hofmann, D. Pfisterer, J. Sann, and B. Meyer, Appl. Phys. A 88, 141 (2007).
- ¹³F. D. Auret, J. M. Nel, M. Hayes, L. Wu, W. Wesch, and E. Wendler, Superlattices Microstruct. 39, 17 (2006).
- ¹⁴M. Diaconu, H. Schmidt, H. Hochmuth, M. Lorenz, H. von Wenckstern, G. Biehne, D. Spemann, and M. Grundmann, Solid State Commun. 137, 417 (2006).
- ¹⁵G. Vincent, A. Chantre, and D. Bois, J. Appl. Phys. **50**, 5484 (1979).
- ¹⁶D. V. Lang, J. Appl. Phys. 45, 3023 (1974).
- ¹⁷Hadia Noor, P. Klason, O. Nur, Q. Wahab, M. Asghar, and M. Willander, J. Appl. Phys. **105**, 123510 (2009).
- ¹⁸D. K. Schroder, Semiconductor Material and Device Characterization, 3rd ed. (Wiley, New York, 2006).
- ¹⁹A. S. Grove, *Physics and Technology of Semiconductor Devices* (John Wiley & Sons, Inc., New York, 1967).
- ²⁰A. Klein, F. Sauberlich, B. Spath, T. Schulmeyer, and D. Kraft, J. Mater. Sci. 42, 1890 (2007).
- ²¹Y. Dong, Z.-Q. Fang, D. C. Look, G. Cantwell, J. Zhang, J. J. Song, and L. J. Brillson, Appl. Phys. Lett. **93**, 072111 (2008).
- ²²Z.-Q. Fang, B. Claffin, D. C. Look, Y. F. Dong, H. L. Mosbacker, and L. J. Brillson, J. Appl. Phys. **104**, 063707 (2008).
- ²³T. Miyajima, K. Akimoto, and Y. Mori, J. Appl. Phys. **67**, 1389 (1990).
- ²⁴N. Baber, H. Scheffler, A. Ostmann, T. Wolf, and D. Bimberg, Phys. Rev. B 45, 4043 (1992).
- ²⁵J. C. Simpson and J. F. Cordaro, J. Appl. Phys. **63**, 1781 (1988).
- ²⁶J. J. Harris, K. J. Lee, J. B. Webb, H. Tang, I. Harrison, L. B. Flannery, T. S. Cheng, and C. T. Foxon, Semicond. Sci. Technol. 15, 413 (2000).
- ²⁷P. Blood and J. W. Orton, The Electrical Characterization of Semiconductors: Majority Carriers and Electron States (Academic, London, 1992).
- ²⁸S. Makram-Ebeid and M. Lannoo, Phys. Rev. Lett. **48**, 1281 (1982).
- ²⁹S. D. Ganichev, E. Ziemann, and W. Prettl, Phys. Rev. B 61, 10361 (2000).
- ³⁰P. A. Martin, B. G. Streetmann, and K. Hess, J. Appl. Phys. **52**, 7409 (1981).
- ³¹S. D. Ganichev, I. N. Yassievich, W. Pettl, J. Diener, B. K. Meyer, and K. W. Benz, Phys. Rev. Lett. **75**, 1590 (1995).

¹D. C. Look, Mater. Sci. Eng. **80**, 383 (2001).

²H. V. Wenckstern, M. Brandt, H. Schmidt, G. Biehne, R. Pickenhain, H. Hochmuth, M. Lorenz, and M. Grundmann, Appl. Phys. A **88**, 135 (2007).